



# Relaxation mechanism of InGaAs single and graded layers grown on (111)B GaAs

T.C. Rojas<sup>a,\*</sup>, S.I. Molina<sup>a,2</sup>, A. Sacedón<sup>b</sup>, F. Valtueña<sup>b</sup>, E. Calleja<sup>b</sup>, R. García<sup>a,3</sup>

<sup>a</sup> Departamento de Ciencia de los Materiales e I.M. y Q.I. Universidad de Cádiz. Apdo. 40, 11510 Puerto Real Cádiz, Spain

<sup>b</sup> Departamento de Ingeniería Electrónica. E.T.S.I. Telecomunicación. Universidad Politécnica de Madrid. Ciudad Universitaria s/n, 28040 Madrid, Spain

## Abstract

In this work we study the influence of the composition (strain) and the layer thickness of InGaAs grown on (111)B GaAs substrates on the surface morphology and defect distribution (strain relief). Samples of uniform ( $x = 0.13$  or  $0.22$ ) and graded ( $x_{\text{initial}} = 0.10$  for each sample;  $x_{\text{final}} = 0.17$  and  $0.25$ ) composition have been studied by scanning electron microscopy (SEM), transmission electron microscopy (TEM) and high resolution electron microscopy (HREM). The relaxation mechanism for the two series of samples is the same. SEM observations reveal a surface roughness with a triangular structure, where the 'cross-hatch pattern' distribution is more isotropic and homogeneous as the thickness and In composition increase. Misfit dislocations and deformation twins (band twins), anisotropically and inhomogeneously arranged, are observed in all the studied samples. Deformation twins are formed by the nucleation of partial dislocations from the film surface. A mechanism of the observed band twins formation is proposed. © 1998 Elsevier Science S.A.

**Keywords:** Composition; InGaAs; Surface morphology

## 1. Introduction

InGaAs/GaAs heterostructures grown on polar orientations exhibit advantages respect to the (100) one, as they permit new optoelectronic applications. Such improvements are due to the large internal electric fields generated by the piezoelectric effect (PF) in coherently strained layers. Among all the polar orientations, the (111) gives the highest PF component perpendicular to the layers [1,2].

To avoid the stacking fault formation during the growth of these structures, it is necessary to tilt the GaAs substrates between  $1\text{--}4^\circ$  towards the [112] direction [3].

To achieve device structures grown on (111)B substrates, it is important to understand the mechanism and stages of mismatch relaxation. This goal requires an accurate control of strain relief, a low threading dislocation density and a flat surface. While for the 'standard' (100)

orientation there are many studies performed, little work has been done for the [111] orientation [4–6].

In this work, we study the influence of In composition ( $x$ ) and layer thickness ( $z$ ) on the surface morphology and defect distribution generated when the strain due to the lattice mismatch between the  $\text{In}_x\text{Ga}_{1-x}\text{As}$  epitaxial layers and the (111)B GaAs substrates is relieved.

## 2. Experimental procedure

Two series of samples have been studied: Series I, uniform composition single layers of  $\text{In}_x\text{Ga}_{1-x}\text{As}$  grown on (111)B GaAs, with  $x = 0.13$  and  $x = 0.22$  with different thickness. Series II, graded composition layers with  $x_{\text{initial}} = 0.10$  and  $x_{\text{final}} = 0.17$  and  $0.25$ .

The growth has been performed by molecular beam epitaxy (MBE). The substrates were disoriented  $1^\circ$  towards the  $[11\bar{2}]$  direction. The remaining growth details for each sample are included in Table 1.

Specimens were prepared to be studied by transmission electron microscopy (TEM) by mechanical thinning followed by  $\text{Ar}^+$  ion milling for cross-sectional observations and by chemical etching ( $\text{H}_2\text{SO}_4 + \text{H}_2\text{O}_2 + \text{H}_2\text{O}$  or  $\text{Br}_2/\text{methanol}$ ) for plan-view orientation. Two of the three

\* Corresponding author.

<sup>1</sup> Fax: +34-56-834924.

<sup>2</sup> Fax: +34-56-834924; e-mail: sergio.molina@uca.es.

<sup>3</sup> Fax: +34-56-834924.

Table 1  
Growth details of the studied samples

Sample	Thickness measured by XTEM (nm)	% In
<i>Uniform composition single layers (series II)</i>		
A	150 ± 4	13
B	260 ± 8	13
C	400 ± 6	14
D	(470–500)	15
E	76 ± 5	21
F	160 ± 6	21
G	240 ± 5	19
H	(270–300)	17.4
<i>Graded composition layers (series II)</i>		
I	240 ± 6	10–17
J	430–460	10–25

possible cross-sections for each sample have been studied.

The techniques used to study the samples were TEM using cross-section (XTEM) and plan-view (PVTEM) orientations, high resolution electron microscopy (HREM) and scanning electron microscopy (SEM). TEM and HREM studies were carried out in the transmission electron microscopes JEOL 1200EX a JEOL 2000 EX, whereas the SEM work was performed with a scanning electron microscope JEOL 820 SM.

### 3. Experimental results

#### 3.1. Surface morphology

Surface morphology has been studied by SEM. Series I samples with the lowest thickness (A and E) have a smooth surface, but random roughness is observed. A tiny cross-hatch triangular pattern with an asymmetric distribution appears, though one of the three expected sets of lines (corresponding to the three  $\langle 110 \rangle$  directions contained in the (111) growth plane) is barely visible (Fig. 1a). As the thickness increases (samples B, C, F and G) a stronger cross-hatch pattern is formed, its distribution is asymmetric and quite inhomogeneous, and there are flat areas surrounded by hatched regions. For samples with the highest thickness (samples D and H) the pattern disposition is more homogeneous, the third set of lines appears, and the ridges run shorter lengths and have complex profiles (Fig. 1b).

Series II samples present a worse surface than the others. A strong triangular cross-hatch pattern visible through the naked eye is observed. The ripples distribution is very asymmetric in sample I as two sets of lines dominate over the third one, but the distribution is more homogeneous. As the In composition and thickness increase (sample J) the pattern is more uniform, the ridges are higher and shorter, and have more complex profiles (Fig. 1c).

#### 3.2. Defect microstructure

XTEM micrographs of the series I samples with the lowest thickness (samples A and E) only show misfit dislocations at the interface and a defect free layer. Samples with thickness  $h > 4h_c$  (samples B, C, D, F, G and H) have misfit dislocations and they show some additional characteristics.

(1) Wide straight contrasts, forming  $110^\circ$  with the interface, which come from the free surface, through the layer and extend deeply into the substrate, and loops of dislocations that look to emanate from the end of these straight lines, connecting and bending towards the interface (Fig. 2a). An adequate contrast diffraction analysis, using large tilt angles, shows that these straight contrasts are dislocation pile-ups, which lie in the same  $\{111\}$  plane (Fig. 2b).

(2) Pile-ups of dislocation half-loops have been observed working with other cross-section orientation. These come from the surface and penetrate deeply into the

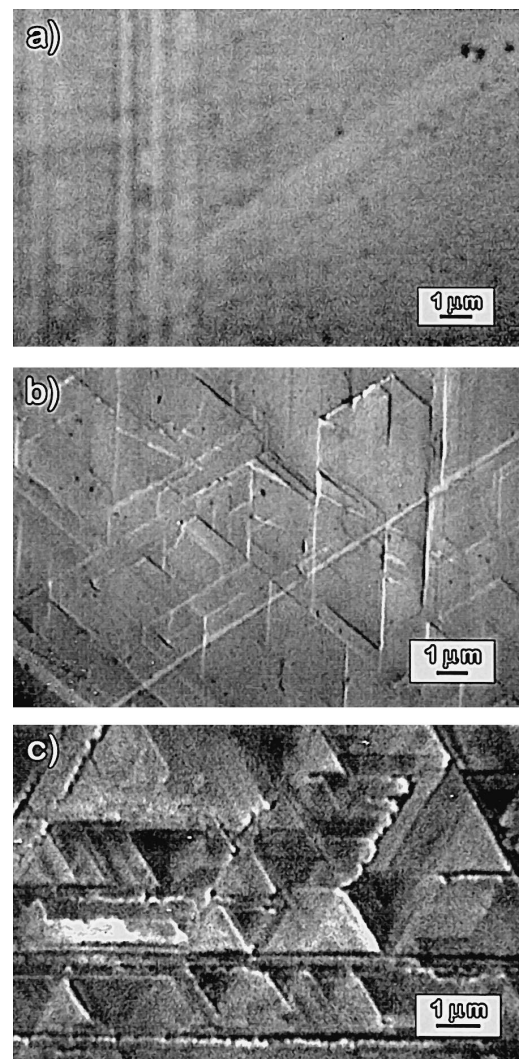


Fig. 1. SEM micrographs from the surface of samples A (a), H (b) and J (c). Micrograph of sample H has been registered tilting the detector  $40^\circ$ .

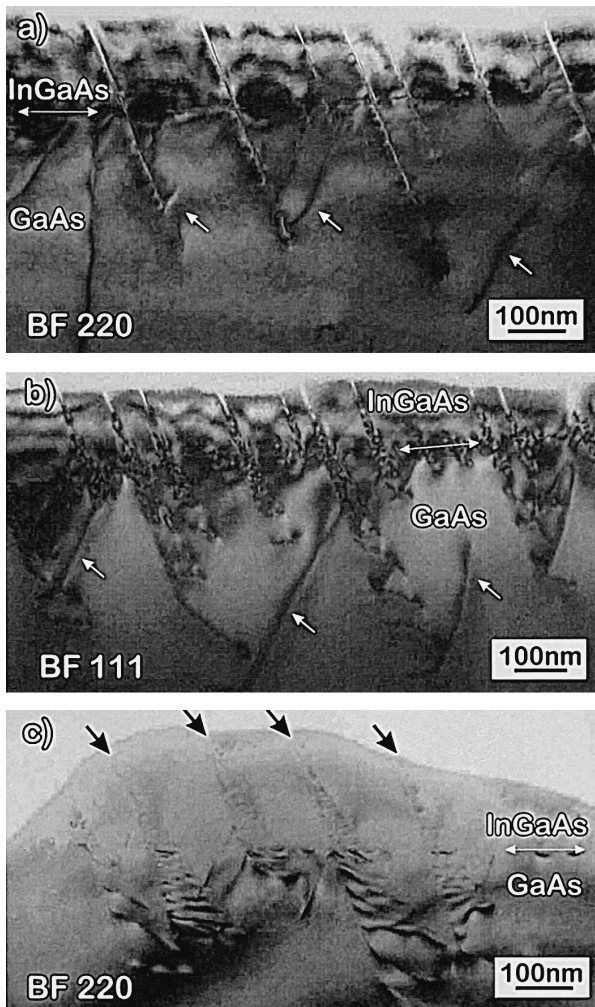


Fig. 2. XTEM images of sample I. (a) Bright Field (BF) image with  $g = 220$ . Dislocations emerging from the twin are arrowed. (b) BF image,  $g = 111$ . Sample has been tilted around the growth direction. (c) BF,  $g = 220$ . This image corresponds to a cross section different from that of (a) and (b).

substrate (1–2  $\mu\text{m}$ ). Standard diffraction contrast experiments have allowed to determine that these dislocations are partial dislocations with the same Burgers vector and lie in the same  $\{111\}$  plane (Fig. 2c).

Plan-view observations on these samples have already been published [4,5]. These works describe the dislocation microstructure and their development as thickness increases, for two uniform composition layers ( $x = 0.12$  and  $0.21$ ). Dislocations that lie inside the layer ('internal' dislocations) are observed to have the form of complex pile-ups lying on the same inclined  $\{111\}$  plane.

The XTEM experimental results of the series II (graded samples) are similar to those of series I (uniform composition samples), but the density of the above explained defects associated to wide straight contrasts is much larger for series II. In this case, it is clearly observed that the straight contrasts are originated at superficial steps, near the troughs of the cross-hatch, formed in the surface.

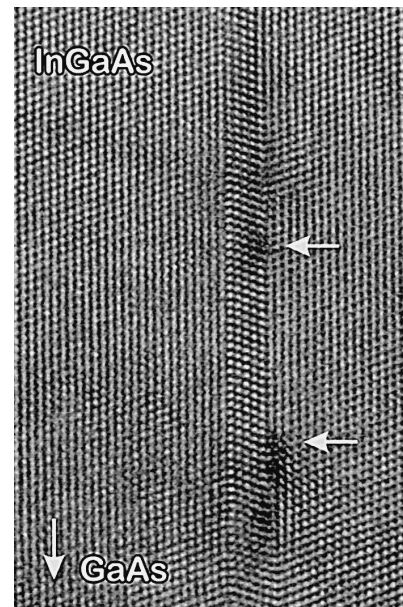


Fig. 3.  $\langle 110 \rangle$  HREM of a twin. Partial dislocations associated to microtwin width changes are arrowed.

The plan-view results are also similar to those obtained on uniform composition layers but the density of misfit and 'internal' dislocations and stacking faults is higher for series II. For this series the defect density increases as the In composition and thickness layer rise. A pile-up of dislocation half-loops, forming a band, and with others half-loops connecting with it, has been detected.

Both groups of samples have been studied by HREM. This study reveals that the straight contrasts observed by XTEM are microtwins. These begin at the surface and penetrate into the substrate. Changes of the twinned plane number into the microtwins are observed along their propagation directions, that is, along the straight contrasts that are extended from the surface up to the interface. Frank partial dislocations are observed to be located just on the zones of change of microtwin widths, as indicated in Fig. 4.

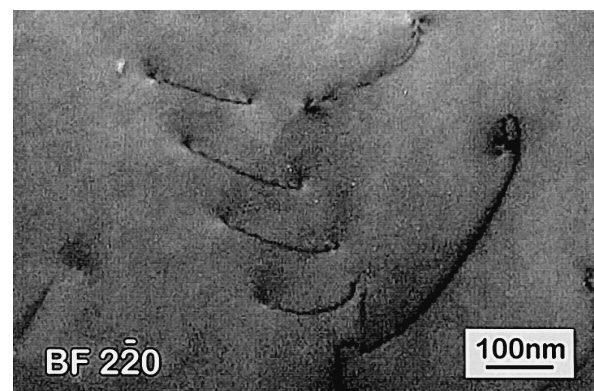


Fig. 4. PVTEM image of sample I,  $g = 2 \bar{2}0$ . The observed dislocation pile-up corresponds to a twin band.

It is worth noting that layer thickness changes of about 30 nm have been measured in samples D, H and J. This is in agreement with the ridge formation at the surface.

#### 4. Discussion

In low lattice-mismatch systems, where coherency stresses can be very large in the strained films, twins may be formed by nucleation of partial dislocations in a {111} plane from the surface, particularly in surface steps. This faulted half-loop increases the step height by a third of the lattice parameter and this step makes the adjacent {111} plane a low energy site for the nucleation of the next partial dislocation half-loop. This process continues until the stress is relieved up to a value below that required for the formation of a critical-size dislocation half-loop. In this way, partial dislocation half-loops with the same Burgers vector form on  $n$  adjacent {111} planes and expand to form a twin band with a thickness  $n \cdot d_{111}$ , where  $d_{111}$  is the {111} interplanar spacing. These twin bands have been observed by Ning et al. [7] in indented films and by Pirouz [8] in heteroepitaxial semiconductors using (001) substrates. These types of twin bands correspond to some of the defects observed by XTEM, PVTEM and HREM (see Fig. 1 Fig. 2–4) in the present work.

Perfect dislocations can be emitted from the incoherent part of an advancing twin front to relieve the long-range stress field of the front [9]. This would explain why we have observed loop dislocations emanating from the twin bands.

On the other hand, the asymmetric distribution of the misfit dislocations [4], and the cross-hatch pattern observed in the first stages of relaxation (this corresponds to samples with the lowest thickness) could explain the asymmetry observed in relation to the twin formation. Nevertheless, more work must be done to confirm this hypothesis.

#### 5. Conclusions

The strain relaxation in uniform and graded composition layers of InGaAs grown on GaAs (111)B substrates

happen by the formation of an asymmetric and anisotropic distribution of misfit dislocations and twin bands. These twin bands are originated by the successive nucleation of partial dislocations in superficial steps and troughs of the cross-hatch pattern. These defects appear for samples with thickness higher than  $4h_c$ .

The surface roughness pattern depends on the thickness and In composition of the InGaAs epilayer. The roughness increases with the epilayer thickness and In composition up to obtain a strong triangular ‘cross-hatch pattern’. The asymmetry and the homogeneity of this pattern have also been found to be dependent on these parameters.

#### Acknowledgements

This work has received financial support of the ‘Comisión Interministerial de Ciencia y Tecnología’ through the project CICYT MAT94-0538 and ‘Junta de Andalucía’ (Group P.A.I. 6020). The work was carried out at the Electron Microscopy Division of the University of Cádiz. The authors would like to thank J.M. Geraldía and M.J. Romero for the technical support during this study. E. Calleja also acknowledges the partial support of CICYT project TIC 95-0770.

#### References

- [1] D.L. Smith, *Solid State Commun.* 57 (1986) 919–921.
- [2] D.L. Smith, C. Mailhot, *Rev. Mod. Phys.* 62 (1990) 173–234.
- [3] K. Yang, L.J. Schowalter, B.K. Laurich, I.H. Campbell, D.L. Smith, *J. Vac. Sci. Technol. B* 11 (3) (1993) 779.
- [4] A. Sacedón, F. Calle, A.L. Alvarez, E. Calleja, E. Muñoz, R. Beanland, P. Goodhed, *Appl. Phys. Lett.* 65 (25) (1994) 1–4.
- [5] R. Beanland, A. Sacedón, E. Calleja, *Inst. Phys. Conf. Ser.* 146 (1995) 169–172.
- [6] T.E. Mitchell, O. Unal, *J. Electron. Mater.* 20 (10) (1991) 723.
- [7] X.J. Ning, T. Perez, P. Pirouz, *Philos. Mag.* A 72 (4) (1995) 837–859.
- [8] P. Pirouz, *Twinning in advanced materials*, in: M.H. Yoo, M. Wuttig (Eds.), *The Minerals, Metals and Materials Society*, Pittsburgh, 1994, pp. 275–295.
- [9] J.P. Hirth, J. Lothe, *Theory of Dislocations*, Wiley, 1982.